

# Study on the Influence of Distribution Lines to Parallel Inverter Systems Adopting the Droop Control Method

Xuan Zhang\*, Jinjun Liu\*, Zhiyuan You†, and Ting Liu\*

\*†Dept. of Electronic Engineering, Xi'an Jiaotong University, Xi'an, China

## Abstract

This paper takes into account the influence of the different impedances of distribution lines on power distribution among inverters when the inverters are paralleled with the droop control method. The impact of distribution lines on the power distribution of inverters can be divided into two aspects. Firstly, since the distributed generators are in low voltage grids, there is resistive impedance in the distribution lines, which will cause control coupling and reduce system stability. The virtual negative resistive impedance of inverters is adopted in this paper to neutralize the resistive element of distribution lines and thus make the distribution line impedance purely inductive. Secondly, after solving the resistive impedance problem, the difference in the inductive impedance value of distribution lines due to the low density of distributed generators will cause an unequal share of reactive power. With regards to this problem, modification is put forward for the droop control strategy to share the reactive power equally. The feasibility of the design is validated by simulation and experimental results.

**Key words:** Distribution line, Droop control, Parallel inverter

## NOMENCLATURE

N	Number of parallel inverters
M	Modulation ratio of an inverter
n	1, ..., N
PCC	Point of Common Coupling
SVG	Static Var Generator
DG	Distributed Generation
DS	Distributed Storage
$P_n$	Output active power of the $n^{\text{th}}$ inverter
$Q_n$	Output reactive power of the $n^{\text{th}}$ inverter
$U_n$	Magnitude (RMS value) of the $n^{\text{th}}$ inverter's output voltage
$I_n$	Magnitude (RMS value) of the $n^{\text{th}}$ inverter's output current
$f_n$	Frequency of the $n^{\text{th}}$ inverter's output voltage
$U_{Dn}$	Voltage on the distribution line connected to the $n^{\text{th}}$ inverter
$U_L$	Magnitude (RMS value) of the voltage at the PCC
$f_L$	Frequency of the voltage at the PCC
$\delta_n$	Angle difference between the $n^{\text{th}}$ inverter's output

voltage and the inverter at the PCC

$k_{pn}$	Gradient of the active power – frequency droop control method
$k_{qn}$	Gradient of the reactive power – magnitude droop control method
$\varphi_n$	Angle difference between the output voltage and the current of the $n^{\text{th}}$ inverter
$R_n$	Resistance in the distribution line connected to the $n^{\text{th}}$ inverter
$L_n$	Inductance in the distribution line connected to the $n^{\text{th}}$ inverter
$L_{fn}$	Inductance of the $n^{\text{th}}$ inverter's low-pass LC filter
$C_{fn}$	Capacitance of the $n^{\text{th}}$ inverter's low-pass LC filter
$R_{fn}$	Resistance in series with $L_f$
$v_n$	Instantaneous value of the $n^{\text{th}}$ inverter's line voltage
$i_n$	Instantaneous value of the $n^{\text{th}}$ inverter's line current
$k_p$	Proportional coefficient of the $n^{\text{th}}$ inverter's PI controller
$k_i$	Integral coefficient of the $n^{\text{th}}$ inverter's PI controller
$R_{Load}$	Resistance of the load paralleling with $L_{Load}$
$L_{Load}$	Inductance of the load paralleling with $R_{Load}$
$X_r$	Rated value of $X$
$X_0$	Value of $X$ at the steady state point
$\hat{x}$	Small-signal perturbation of $X$

Manuscript received Oct. 31, 2012; revised Apr. 15, 2013

Recommended for publication by Associate Editor Kyeon Hur.

†Corresponding Author: flyaway.yuan@qq.com

Tel: +86-158-2930-5966, Xi'an Jiaotong University

\*Dept. of Electronic Engineering, Xi'an Jiaotong University, Xi'an, China

$X^*$  Reference value of  $X$   
 $\vec{X}$  Vector  $X$   
 $X^{(k)}$  Value of  $X$  after the  $k^{\text{th}}$  time iteration

## I. INTRODUCTION

Parallel connection is an important method of power distribution. The control methods of parallel inverters can be divided into parallel connections with control interconnections and without control interconnections. In a parallel inverter system with control interconnections, the control methods of the power distribution include the master slave mode, central type and wraparound type [1]-[3]. Their advantage lies in the rapid power sharing speed. However, they also have disadvantages. The cost of system manufacturing is high due to the control interconnections, and they are easily affected by high frequency interference since the control interconnection lines are quite long in the application of distributed power generation. The control method without control interconnections is the droop control method. Since the output voltage reference is produced by the parallel inverter itself, control interconnections are not necessary. This reduces the system manufacturing costs and avoids the interference from the control interconnection lines [4], [5]. However, one of its disadvantages is that as the load becomes different, a shift of voltage may occur. The authors of [6], [7] have researched this disadvantage. Another disadvantage is that because the power sharing mechanism is in a power loop outside the voltage loop, the power sharing speed is slow. This defect can be resolved by having the differential and integral processing of the power carried out in the droop control method [8].

In recent years, since renewable energy resources and distributed power generation have become widely used, the distance between inverters and load has become varied. Thus the characteristics of the distribution lines has to be taken into account, which brings new problems to the droop control method. The impact of distribution lines has two different cases.

Firstly, since generators with inverters are in a low voltage grid, there is a resistive impedance in the distribution line, which will cause control coupling. This in turn affects the dynamic response and reduces system stability. Secondly, the difference in the value of the distribution lines' inductive impedance due to the low density of the distributed generators will cause an unequal share of reactive power.

[9] considered the effect of the line impedance in parallel inverters. However, how the line impedance affects power distribution had not been realized thoroughly, so the proposed method is complex and the results were not perfect. Methods which increase the output impedance of each parallel inverter were proposed in [10]-[12] to ignore the influence of the distribution lines. These methods are simple and practical, but they reduce the response time of systems. An improved droop controller was proposed in [13] to achieve accurate power sharing by introducing the PCC's voltage feedback. However,

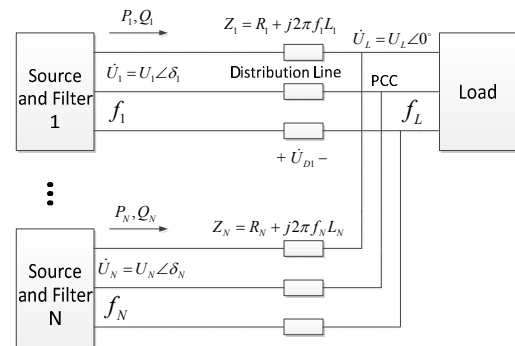


Fig. 1. The schematic diagram of N inverters supplying power through distribution lines.

in practice, it is difficult to measure the PCC's voltage since the distribution lines may be long. Methods of rotating the droop control coordinates were adopted in [14], [15] to decouple the active and reactive control. These control methods can resolve the problems caused by the resistance in distribution lines. However, it cannot share power equally when the resistive components in every distribution line are different.

To solve the coupling problem caused by the resistance in distribution lines, a control method is proposed to make the equivalent output impedance of the inverter negatively resistive, the value of which is identical to the resistance in the distribution line connected to the inverter. As a result, the overall impedance on the distribution lines can be treated as pure inductive, which means that the control coupling caused by the resistance in distribution lines no longer exists. The problem is then transformed into a condition where the distribution line is characterized by pure inductance. However, differences in the impedance value result in unequal sharing of the reactive power even when the inverters are using the same droop control method. A modified droop control method, in which the output reactive power of each inverter is related to the voltage at the PCC instead of the voltage at the inverter output terminal, with the proposed indirect voltage control method to equally distribute the reactive power. The voltage at the PCC is unique. As a result, the reactive power can be equally shared when the parallel inverters are using the same modified droop control method.

## II. MODIFICATION OF THE DROOP CONTROL STRATEGY TO SOLVE THE COUPLING ISSUE

### A. Coupling Caused by Resistance in Distribution Lines

DGs and loads are widely distributed, but generally they are connected to one bus through distribution lines. Because there is a long distance from the bus, the voltage drop on the bus can be neglected when compared with the voltage drop on the distribution lines. Therefore, it can be that every inverter is connected to the PCC through the distribution line [16]-[18]. The circuit diagram is shown in Fig. 1.

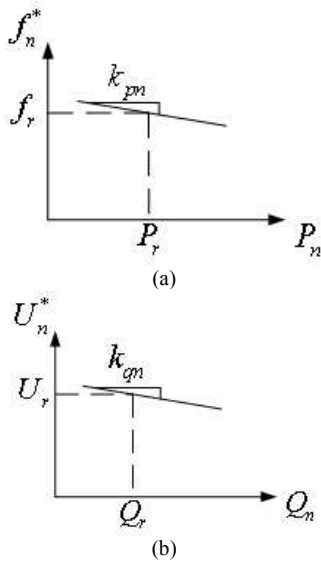


Fig. 2. The schematic diagram of the droop control method (a) Active-frequency droop control (b) Reactive- magnitude droop control

The output active power and reactive power of the arbitrary  $n^{\text{th}}$  inverter are [19]:

$$P_n = \frac{U_n^2 \cos \delta_n - U_n U_L \cos(\delta_n + \gamma_n)}{Z_n} \quad (1a)$$

$$Q_n = \frac{U_n^2 \sin \delta_n - U_n U_L \sin(\delta_n + \gamma_n)}{Z_n} \quad (1b)$$

Where:

$$Z_n = \sqrt{(2\pi f_n L_n)^2 + R_n^2}$$

$$\gamma_n = \arctan \frac{2\pi f_n L_n}{R_n}$$

If the generators are in a transmission network,  $2\pi f_n L_n$  is much larger than  $R_n$ . Therefore,  $\gamma_n$  is approximately equal to  $\pi/2$ . As a result, (1) can be simplified as (2).

$$P_n = \frac{U_n U_L}{2\pi f_n L_n} \sin \delta_n \quad (2a)$$

$$Q_n = \frac{U_n (U_n - U_L \cos \delta_n)}{2\pi f_n L_n} \quad (2b)$$

It can be obtained from (2) that the active power is proportional to the voltage angle difference and the reactive power is proportional to the voltage magnitude difference, considering that  $\delta_n$  is generally quite small,  $\sin \delta_n \approx \delta_n$ , and  $\cos \delta_n \approx 1$ . Considering that the angle difference can be adjusted by the frequency, the two control closed loops, namely the droop control method, can be formed to distribute the active and reactive power, respectively, which can be expressed as (3). In the droop control method for an arbitrary  $n^{\text{th}}$  inverter, the relationship between the power and voltage frequency as well as the magnitude references are shown in Fig. 2[20].

$$f_n^* - f_r = -k_{pm} \left( \frac{\omega_c}{s + \omega_c} P_n - P_r \right) \quad (3a)$$

$$U_n^* - U_r = -k_{qm} \left( \frac{\omega_c}{s + \omega_c} Q_n - Q_r \right) \quad (3b)$$

In that condition, when the reactive power changes, the amplitude of the voltage also changes, which will affect the active power. However, this is a one-way influence that can be solved by using a reactive power compensator, such as a SVG.

However, with the development of distributed generation, there are more and more generators in the power distribution network, in which  $R_n$  cannot be neglected. If the droop control method of (3) is adopted, it can be seen from (1) that the change of phase angle influences not only the active power but also the reactive power. Similarly, the change of the magnitude difference also influences both the active power and the reactive power. As a result, the coupling makes the transient process slow and reduces the system stability. Therefore the predetermined target cannot be reached through the droop control method.

### B. The Application of Virtual Negative Resistive Impedance in the Droop Control Method

According to the analysis above, it is  $R_n$  that impacts the control effect. Therefore, the basic idea to solve this problem is to cancel out  $R_n$  in the equivalent circuit by changing the output impedance of the  $n^{\text{th}}$  inverter into  $-R_n$ . To realize this control target, the original output impedance of the inverter has to be studied first.

In a parallel inverter system, the control and main circuits of one parallel branch are shown in Fig. 3. It can be seen that there are two control loops in the control circuit. The outer loop is the droop control, the aim of which is to obtain the voltage reference, and the inner loop is the voltage loop, the aim of which is to output the voltage following its reference. For the voltage loop, three PI controllers are used for each phase. The block diagram of ‘‘Sine Wave Generator’’ can be expressed as:

$$v_{in}^* = \begin{bmatrix} v_{abn}^* \\ v_{bcn}^* \\ v_{can}^* \end{bmatrix} = U_n^* \begin{bmatrix} \cos(2\pi f_n^* t) \\ \cos\left(2\pi f_n^* t - \frac{2\pi}{3}\right) \\ \cos\left(2\pi f_n^* t + \frac{2\pi}{3}\right) \end{bmatrix}$$

The main and control circuit block diagram of the three-phase inverter is shown in Fig. 4[10] to obtain the output impedance. The outer loop is ignored while observing the output impedance, because the output impedance is irrelevant to the change of the voltage reference.

According to Fig. 4, the closed loop voltage gain  $G$  and output impedance  $Z_o$  of the  $n^{\text{th}}$  inverter can be obtained as:

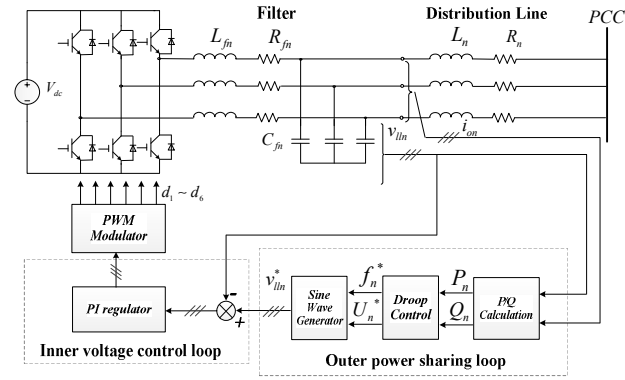


Fig. 3. The schematic diagram of one parallel inverter adopting the droop control method.

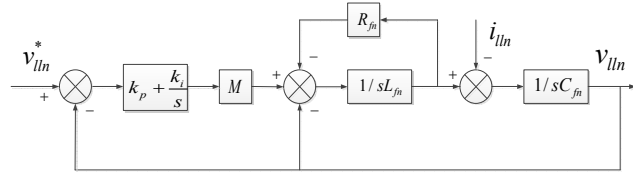


Fig. 4. The main and control circuit of a voltage source inverter (VSI).

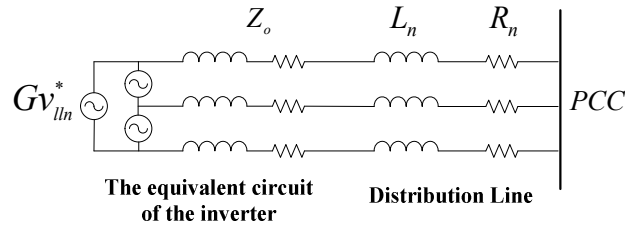


Fig. 5. The equivalent circuit of inverters supplying power through resistive and inductive distribution line.

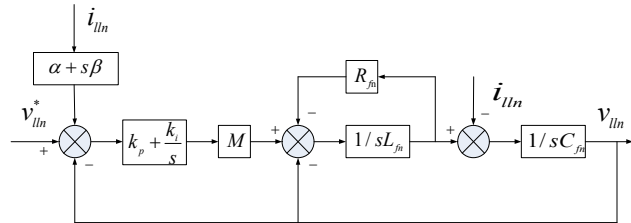


Fig. 6. The main and control circuit of a VSI with negative resistive output impedance.

$$\left. \begin{aligned}
 G &= \frac{v_{lln}}{v_{lln}^*} \Big|_{i_{lln}^* = 0} \\
 &= \frac{k_p Ms + k_i M}{L_{fn} C_{fn} s^3 + R_{fn} C_{fn} s^2 + (k_p M + 1)s + k_i M} \quad (4) \\
 Z_o &= \frac{v_{lln}}{i_{lln}^*} \Big|_{v_{lln}^* = 0} \\
 &= \frac{L_{fn} s^2 + R_{fn} s}{L_{fn} C_{fn} s^3 + R_{fn} C_{fn} s^2 + (k_p M + 1)s + k_i M}
 \end{aligned} \right\}$$

According to (4), the equivalent circuit of the inverter connected to the distribution line can be obtained and is shown in Fig. 5.

In Fig. 5, the equivalent output impedance  $Z_o$  is approximately inductive at the power frequency and its

amplitude can be neglected when compared with that of the distribution line. A modified control method for the inverters is proposed to change the equivalent output impedance, shown in Fig. 6.

At this time, the equivalent output impedance of the  $n^{th}$  inverter is:

$$\begin{aligned}
 Z_{og} &= \frac{v_{lln}}{i_{lln}^*} \Big|_{v_{lln}^* = 0} \\
 &= \frac{(k_p \beta M + L_{fn})s^2 + (k_p \alpha M + k_i \beta + R_{fn})s + k_i \alpha M}{L_{fn} C_{fn} s^3 + R_{fn} C_{fn} s^2 + (k_p M + 1)s + k_i M} \quad (5)
 \end{aligned}$$

In order to make the modified equivalent output impedance resistive and to ensure that the value is equal to that of the distribution line at the power frequency (50Hz), it is assumed that:

$$Z_{og} \Big|_{s=j100\pi} = -R_n \quad (6)$$

Substitute (6) into (5) to obtain the expression of  $\alpha$  and  $\beta$  in fig. 5:

$$\begin{aligned}
 \alpha &= \frac{A\omega^2 k_p - Bk_i}{(k_i^2 + \omega^2 k_p^2)M} \\
 \beta &= \frac{Ak_i + Bk_p}{(k_i^2 + \omega^2 k_p^2)M}
 \end{aligned}$$

Where:

$$A = (k_p M - L_{fn} C_{fn} \omega^2 + 1)R_n + R_{fn}$$

$$B = k_i M + (R_{fn} R_n C_{fn} + L_{fn})\omega^2$$

$$\omega = 2\pi * 50$$

After being modified according to Fig. 6, the equivalent circuit is shown in Fig. 7.

It can be seen from Fig. 7 that the equivalent circuit has changed so that the inverters supply power to the load through a purely inductive distribution line. Thus the coupling caused by the resistive part of the distribution line no longer exists. As a result, the droop control method can still be adopted to distribute power.

Usually, an inner current loop is added in the control strategy. In that situation, the intrinsic inertial element,  $1/(sL_{fn} + R_{fn})$ , will change into a smaller inertial element with a higher cutoff frequency. As a result, the dynamic performance of the inverter is improved. The form of an equivalent circuit with the current loop is similar to Fig. 4, and the procedure for obtaining the negative resistive impedance is the same as that introduced in this section.

After cancelling the resistive part of the distribution line, the inductive impedance value difference of the distribution lines due to the low density of the distributed generators and the different lengths will cause an unequal share of the reactive power when the traditional droop control method is adopted.

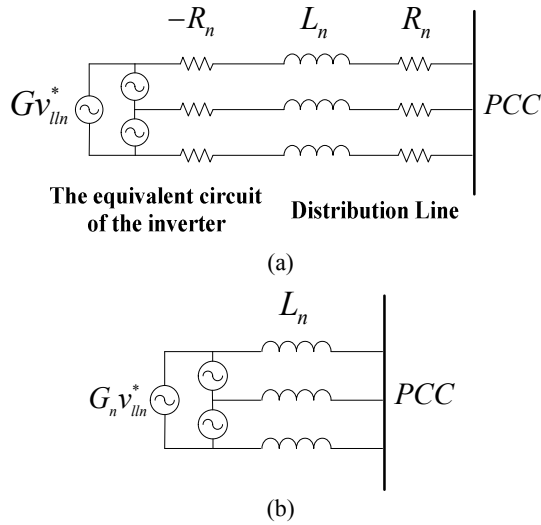


Fig. 7. The equivalent circuit of an parallel branch (a) The output impedance of the  $n$ th inverter is characterized by negative resistance (b) The equivalent circuit after the cancellation between virtual impedance and distribution line resistance

### III. MODIFICATION OF THE DROOP CONTROL STRATEGY TO SOLVE THE POWER SHARING ISSUE

#### A. Influence of Different Inductances of Distribution Lines on the Power Sharing of Parallel Inverters

After solving the coupling problem caused by  $R_n$ , the distribution lines can be considered to be pure inductive, that is  $R_n = 0\Omega$ , and the output power of the inverters can be expressed as (2):

$$P_n = \frac{U_n U_L}{2\pi f_n L_n} \sin \delta_n \quad (2a)$$

$$Q_n = \frac{U_n (U_n - U_L \cos \delta_n)}{2\pi f_n L_n} \quad (2b)$$

This can be obtained through Fig.1

$$\frac{d\delta_n}{dt} = 2\pi(f_n - f_L) \quad (7)$$

When the parallel system is in the steady state, all of the parameters in (6) are constant. This means that  $\delta_n$  in (7) is constant. Thus it can be obtained by:

$$f_1 = \dots = f_N = f_L \quad (8)$$

This indicates that the output voltage frequencies of all the inverters are identical in steady state. If the droop control method in (2a) is used in every inverter, (9) can be derived after substituting (8) into (2-a).

$$P_1 = P_2 = \dots = P_N \quad (9)$$

The above analysis is independent of the impedance amplitude of the distribution lines. This demonstrates that when the distribution lines of the inverters are different in size and the same droop control strategy is adopted, the active power is still equally distributed.

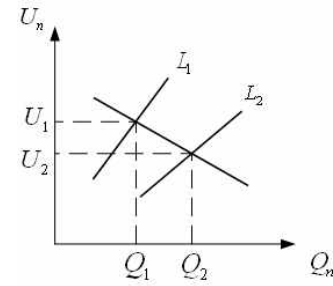


Fig. 8. The Q-U relationships of control and main circuits.

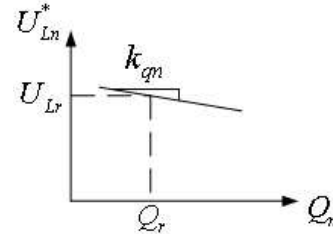


Fig. 9. The modified Q-U droop control method.

It can be seen from (2-b) that when the impedances of the distribution lines are different, supposing  $N=2$  and  $L_1 > L_2$ , the relationship between the reactive power and the inverter output voltage is shown as Fig. 8. It can be seen from Fig. 8 that when the impedance of the distribution lines is different, the two inverters have two different steady working points. This indicates that when the two inverters adopt the same droop control method, their output reactive power are not equal and the one with a larger distribution line impedance outputs a lower reactive power.

#### B. Modification of the Reactive-Magnitude Droop Control Method

It can be seen from Fig. 1 that two inverters are connected to the same point (PCC) through the distribution lines. Therefore, the control strategy of the droop control method is changed from obtaining the inverter's output voltage magnitude reference to obtaining the PCC's voltage magnitude reference on the basis of the reactive power. The control strategy can be shown in Fig. 9 and the equation of the control circuit is:

$$U_{Ln}^* - U_{Lr} = -k_{qm} \left( \frac{\omega_c}{s + \omega_c} Q_n - Q_r \right) \quad (10)$$

Because the inverters are connected to the same terminal, as shown in Fig. 1, and use the same droop control method, expressed as (10), the voltage reference in the steady state is equal to its actual value. This can be expressed as:

$$U_{L1}^* = U_{L2}^* = \dots = U_{LN}^* = U_L \quad (11)$$

By substituting (11) into (10), it can be obtained that:

$$Q_1 = Q_2 = \dots = Q_N \quad (12)$$

(12) indicates that if parallel inverters use the same modified droop control method, expressed as (10), and then realize the control target, expressed as (11), the output reactive power can be shared equally.

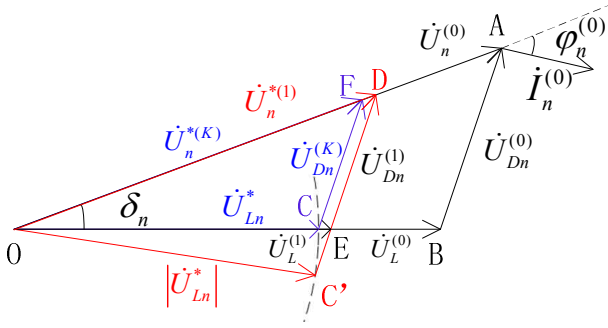


Fig. 10. Vector diagram of indirect voltage control.

However, the voltage magnitude reference at the PCC cannot be used to control an inverter directly. Here a control method, namely indirect voltage control, is proposed to obtain the output voltage magnitude. The indirect voltage control can be expressed as (13), which is derived by the cosine law.

$$U_n^* = \sqrt{U_{Ln}^{*2} - (Z_n I_n \cos \varphi_n)^2} + Z_n I_n \sin \varphi_n \quad (13)$$

Next, a transient process is analyzed as an illustration of the indirect voltage control. In Fig. 10, when the system in Fig. 1 is in the original state, the voltage vectors  $\dot{U}_n^{(0)}$ ,  $\dot{U}_{Dn}^{(0)}$  and  $\dot{U}_L^{(0)}$  form a triangle  $\triangle OAB$  according to the KVL, in which  $\dot{U}_{Dn}^{(0)}$  is  $\pi/2$  phase advance  $\dot{i}_n^{(0)}$ , and the length of  $\dot{U}_{Dn}^{(0)}$  is  $Z_n I_n$ . Considering that the angle difference  $\delta_n$  is determined by the P-f droop control method, expressed as (2-a),  $\delta_n$  is assumed to be constant in the following transient process.

Assuming that the magnitude of the PCC's voltage  $\dot{U}_{Ln}^*$  is reduced to  $\overline{OC'}$  by the modified droop control method in (10), a new triangle  $\triangle OC'D$  is designed by knowing two sides and one angle, as shown in (14).

$$\begin{cases} \overline{OC'} = |\dot{U}_{Ln}^*| = \overline{OC} \\ \overline{C'D} = |\dot{U}_{Dn}^{(K)}| = \overline{AB} \\ \angle ODC = \angle OAB = 90^\circ - \varphi_n^{(0)} \end{cases} \quad (14)$$

The third side  $\overline{OD}$  which can be derived by (13) is used as  $\dot{U}_n^{(1)}$ . A typical cosine law form with an iteration of (13) can be written as (15).

$$\begin{aligned} (U_{Ln}^*)^2 = & (U_n^{*(k)})^2 + (U_{Dn}^{(k-1)})^2 \\ & - 2U_n^{*(k)}U_{Dn}^{(k-1)} \cos\left(\frac{\pi}{2} - \varphi_n^{(k-1)}\right) \end{aligned} \quad (15)$$

Then after the modulation of the voltage loop, the output voltage of the inverter  $\dot{U}_n^{(1)}$  is equal to its reference  $\dot{U}_n^{*(1)}$ , and  $\dot{U}_n^{(1)}$ ,  $\dot{U}_{Dn}^{(1)}$  and  $\dot{U}_L^{(1)}$  form a new triangle  $\triangle ODE$  according to the KVL. It can be observed that  $\dot{U}_L^{(1)}$  approaches its reference after one iteration. Then,  $\dot{U}_{Ln}^*$  and the renewed  $\dot{U}_{Dn}^{(1)}$  are used again to get  $\dot{U}_n^{*(2)}$  by using (15). After several iterations,  $\dot{U}_L^{(K)}$  will equal to  $\dot{U}_{Ln}^*$ , and the steady state  $\triangle OFC$  will eventually be realized.

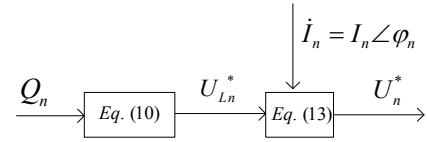


Fig. 11. The control block diagram of modified Q-U droop control method.

As can be seen from the above analysis, when the indirect voltage control method is used, during the transient process, the final reference of the output voltage magnitude  $U_n^{*(K)}$  cannot be derived at the beginning of the transient process. However, the introduced current closed loop can make the control system achieve the final target.

The influence on the stability of the voltage loop after introducing the indirect voltage control is also theoretically analyzed. If it is assumed that the transfer function of the inverter output voltage loop can be expressed as (16), a first-order inertia process with the time constant  $T$ , the transfer function of the PCC voltage loop can be derived, which can be expressed as (17):

$$\hat{u}_n = \frac{\hat{u}_L^*}{1 + Ts} \quad (16)$$

$$\frac{\hat{u}_L}{\hat{u}_{Ln}^*} = \frac{1}{(1 + C \sin \varphi_n \sqrt{1 - C^2 \cos^2 \varphi_n} - C^2 \cos^2 \varphi_n)Ts + 1} \quad (17)$$

In which  $C = 2\pi f L_n / N Z_{Load}$ .

The deduction of (17) is in Appendix I. From (17), it can be seen that introducing the indirect voltage control keeps the system stable, and since  $C$  and  $\varphi_n$  in (17) are both close to 0, the time constant barely increases.

The control block diagram of the modified Q-U droop control method with indirect voltage control is shown in Fig. 11.

When the distribution line is characterized by pure inductance but various in size, the active power is equally distributed, and the reactive power is not equally shared when the inverter is connected in parallel. This has been analyzed and a set of solutions has been put forward by the above analysis.

#### IV. SIMULATION AND EXPERIMENTAL VALIDATION

Two 10kVA parallel three phase inverters were taken as the experiment platform, and the main circuit was constructed as in Fig. 1. Both inverters used a DSP28335 as their central processing unit, and the switching frequency of the IGBTs is 10kHz under normal operating conditions. The other parameters of the main and control circuit are shown in table I.

##### A. Case 1 The traditional droop control method with SPWM

When the traditional droop control method is adopted, the

TABLE I

SIMULATION AND EXPERIMENT PARAMETERS OF INVERTERS IN MAIN AND CONTROL CIRCUIT

CASE 1 & 2 :		CASE 3 : 0.8	
$L_1(\text{mH})$	2.8	$L_2(\text{mH})$	2.8
$R_1(\Omega)$	1	$R_2(\Omega)$	1
$k_{q1}(\text{V/Var})$	$5 \cdot 10^{-3}$	$k_{q2}(\text{V/Var})$	$5 \cdot 10^{-3}$
$k_{p1}(\text{rad/W*s})$	$4 \cdot 10^{-5}$	$k_{p2}(\text{rad/W*s})$	$4 \cdot 10^{-5}$
$P_r(\text{W})$	2000	$Q_r(\text{W})$	2000
$R_{load}(\Omega)$	Light load: 25 Heavy load: 8	$L_{load}(\text{mH})$	60
$U_{Lr}(\text{V})$	200	$f_r(\text{Hz})$	50

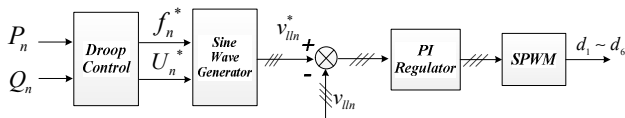


Fig. 12. The control block diagram of Case 1.

control block diagram is shown in Fig. 12. Under this control method, when the distribution lines are equal and without a resistance component, the output powers of each inverter are shown in Fig. 13. It can be seen that both the active and reactive powers are equally distributed under both light load and heavy load situations.

If the distribution lines are resistive-inductive, the power distribution situations are shown in Fig. 14. Fig. 14(a) shows the situation where the load increases to a heavy load, from which it can be observed that the active power and reactive power tend to be stable but the transient process is slower and the circulating current is larger when compared with the situation in Fig. 13. In Fig. 14(b), the disturbance is increased until the inverter is vibrated to stop when the inverter decreases from a heavy load to a light load.

A. Case 2 The Traditional Droop Control Method with Virtual Negative Resistance Impedance

In this case, the control block diagram is shown in Fig. 15.

The output impedances, before and after the change, is shown in Fig. 16.  $Z_o$  in Fig.16 refers to the output impedance when the control mode in Fig. 4 is adopted, and  $Z_{og}$  refers to the output impedance when the control mode in Fig. 6 is adopted. It can be seen from the figure that when the line frequency is 50Hz, the  $Z_o$  magnitude is -20dB and the phase angle is approximately 90 degrees. This indicates that when the

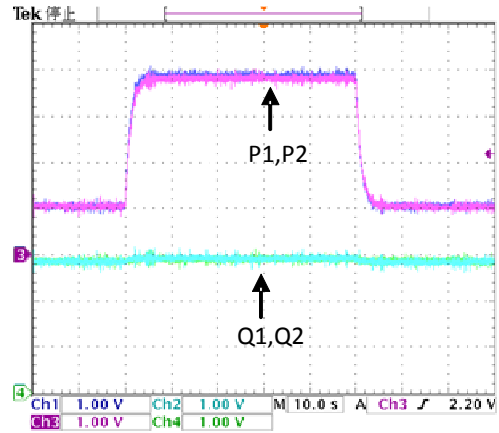
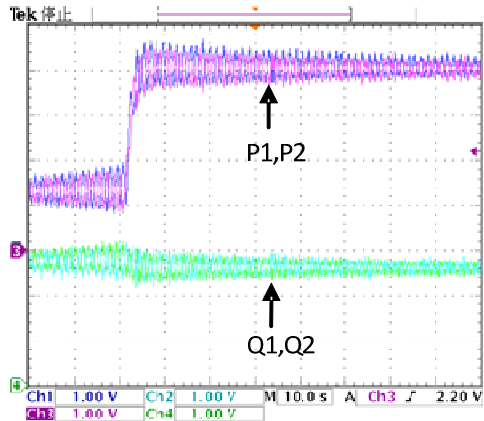
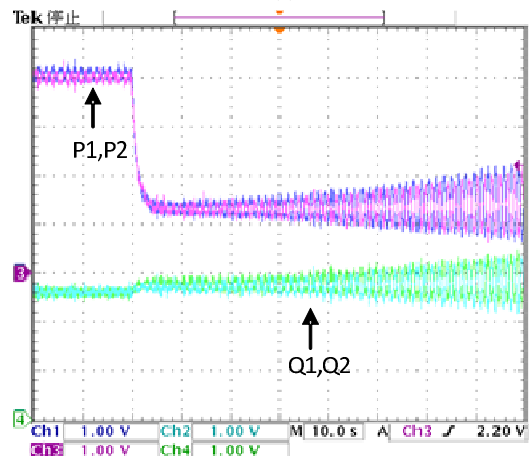


Fig. 13. Power distribution when the distribution lines are characterized by pure equal inductances



(a)



(b)

Fig. 14. Power distribution with resistances in distribution lines (a) The load increases from light to heavy (b) The load decreases from heavy to light.

normal voltage loop control is adopted, as shown in Fig. 4, the output impedance of the inverters is close to the series connection between the inductance and the resistance and is basically characterized by the inductance. The magnitude of  $Z_{og}$  at line frequency 50Hz is 0dB and the phase angle is 180 degrees. This indicates that the output impedance at this



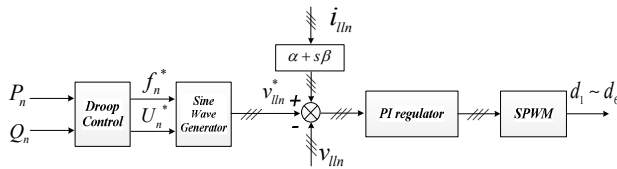


Fig. 15. The control block diagram of Case 2

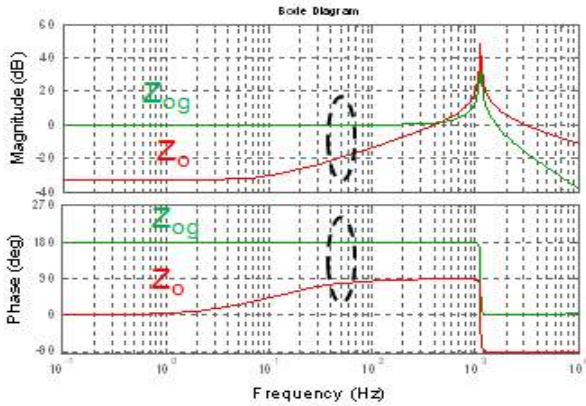


Fig. 16. Output impedance of an inverter before and after introducing virtual negative resistive impedance

frequency has changed to  $-1\Omega$  which is equal to the resistive parts of the distribution line, listed in table I, in magnitude but opposite in direction.

Fig. 17 shows the power sharing situation of the two inverters after the virtual negative resistive impedance is adopted. It can be seen from Fig. 17(a) that the power sharing effect is identical to the effect of the situation where the distribution line is characterized by pure inductance, as shown in Fig. 13. Fig. 17(b) shows that the control strategy changes to the droop control method with a virtual negative resistive impedance from the conventional droop control method at 10s. It can be seen from the figure that the disturbance in the output power disappears after the control strategy is switched.

Fig. 18 shows the power distribution of the two inverters adopting only the droop control with a virtual negative resistive impedance when the distribution lines are resistive-inductive but with different values. Although the stability issue caused by the resistance in the distribution lines is eliminated, the problem of power sharing still exists.

Fig. 18(a) shows the *a* phase currents of the two inverters, and Fig. 18(b) is the active power and reactive power of each inverter. It can be seen from table I that the same droop control curve is adopted by the two inverters. However, 18(a) shows that the two inverters do not share the same current. A clearer conclusion can be obtained from 18(b): the active power of the two inverters is not influenced by different inductance values. Because their droop control curves are identical, the active power is equally distributed. However, the reactive power is not equally distributed, and the reactive power of the inverter with a larger distribution line impedance is smaller. These conclusions are consistent with the analysis in III.A.

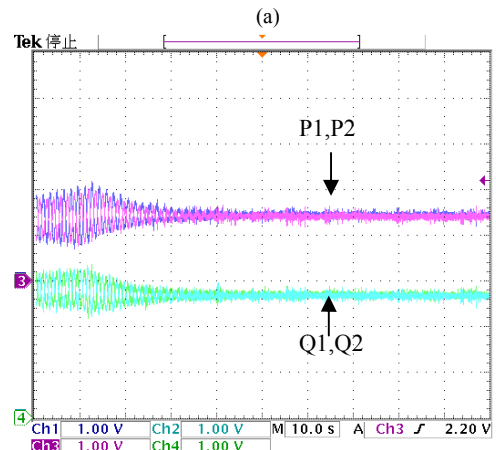
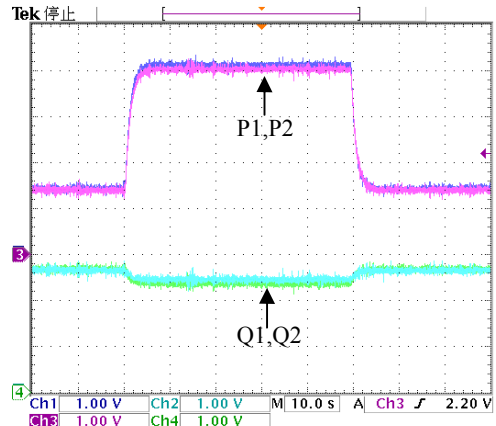


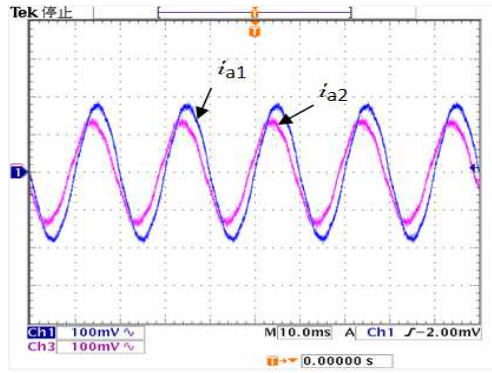
Fig. 17. Power sharing character under the droop control method with virtual negative resistive impedance (a) Power sharing when the load changes (b) Power sharing before and after the change of strategy.

*B. Case 3 The Modified Droop Control Method with Indirect Voltage Control and a Virtual Negative Resistive Output Impedance*

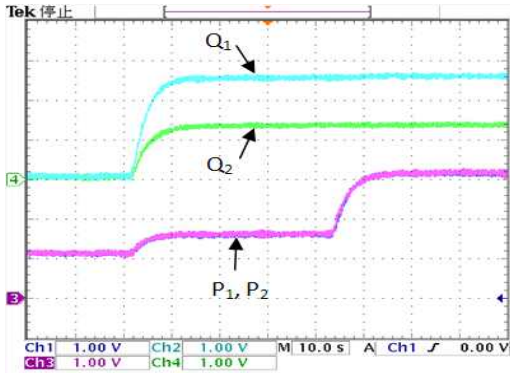
In this case, the control block diagram is shown in Fig. 19. In this figure,  $f_n^*$  is formed by the traditional droop control and  $U_n^*$  is formed by the modified droop control with indirect voltage control. After  $v_h^*$  is derived by  $f_n^*$  and  $U_n^*$ , the virtual negative resistive impedance is applied in the voltage loop.

First, the principle of the indirect voltage control is verified. Fig. 20 shows the transient process of the indirect voltage control by simulation. When the reactive load increases,  $U_{Ln}^*$  decreases, according to the droop control method. The blue and green curves in this figure show  $U_n^*$  obtained by (13) and  $U_{Ln}^*$  obtained by (10), respectively. The cyan and red curves represent  $U_n$  and  $U_L$ , respectively. It can be seen from Fig. 20 that when  $U_{Ln}^*$  decreases,  $U_n^*$  also decreases, and  $U_L$  follows  $U_{Ln}^*$  as  $U_n$  follows  $U_n^*$ . The time constants of the two transient processes,  $U_L$  and  $U_n$ , are basically the same as the former but slightly larger than the latter. This is consistent with





(a)



(b)

Fig. 18. Power sharing character under the droop control when distribution lines are different (a) A-phase current of the two inverters (b) Active power and reactive power of the two inverters.

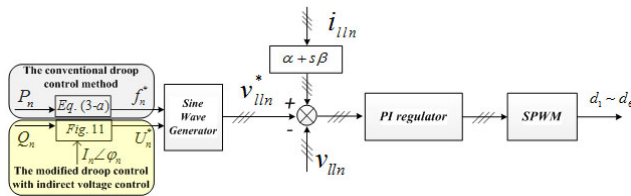


Fig. 19. The control block diagram of Case 3.

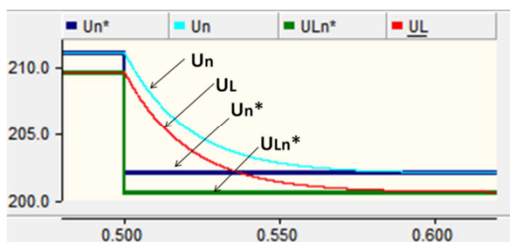
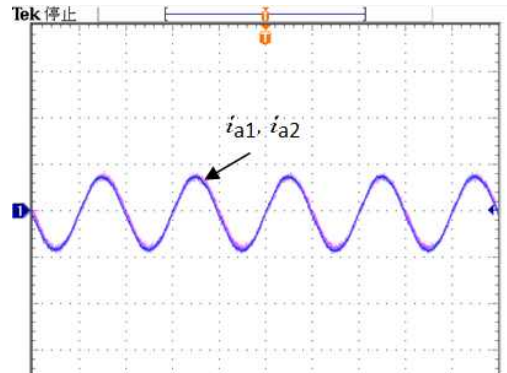


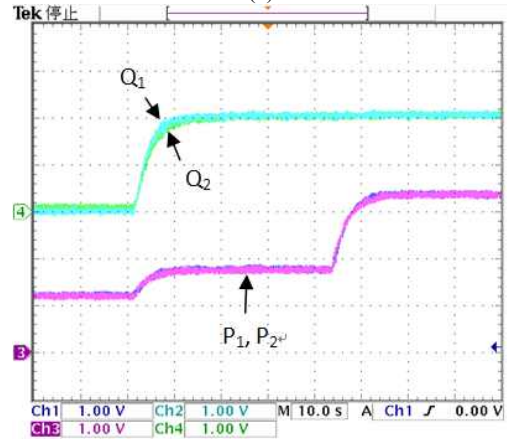
Fig. 20. The simulation result of transient process and stability of indirect voltage control.

the conclusion, (16) and (17), obtained from the stability analysis.

Fig. 21 shows the power distribution situation with the control method in Fig. 19, when there are resistances in the distribution lines and the inductances are different. Fig. 21(a) shows that the currents of the two inverters are equal. Fig. 21(b) shows the equal distribution of the active power and that of the



(a)



(b)

Fig. 21. Power sharing character under the modified droop control when distribution lines are different (a) A-phase current of the two inverters (b) Active power and reactive power of the two inverters.

reactive power. This means that, in addition to solving the stability issue, the problem of an unequal share of power brought by different impedances in the distribution lines can also be effectively solved by the modified droop control method with indirect voltage control.

## V. DISCUSSION

If the rated capacities of the inverters are different, such as x:1 for a two parallel inverter system, the ratio of the output powers also should be x:1. Under this condition, the P-f droop control strategy can be shown in Fig. 22. The situation of the Q-U droop control method is similar. However, the couple issue and the power sharing issue caused by the distribution line still exists. The analysis and discussion in this paper is under the condition that the inverters have the same capacity for better understanding. The proposed strategies are also suitable when the capacities of the inverters are different.

To solve the problem of power distribution among parallel inverters caused by distribution lines, control strategies are proposed aiming at control coupling and power sharing

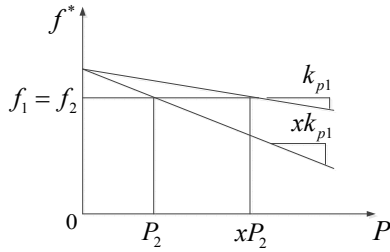


Fig. 22. The P-f droop control strategy when the capacities of parallel inverters are different.

unequally. In these proposed control strategies, the impedance of the distribution lines should be required first. Some mature techniques have been proposed to meter the impedance of distribution lines [21]–[24]. This makes these proposed control strategies feasible. Moreover, because a slight control coupling barely affects the stability of a parallel system, and a slight unequal power sharing is also affected by the parallel inverters themselves, the requirement of the precision of the distribution line's impedance is not rigorous in the proposed control strategies. This means that the impedance of the distribution line does not have to be real-time metered. Therefore, after metering the resistance and inductance of the distribution line, these values can be put into the controller of the inverter as constant parameters before the inverter works in the grid. Like the traditional droop control strategy, no extra coordinate control unit or inter connection among the inverters is used while the system is running.

In addition, for the control coupling situation, the modification is in the voltage loop after obtaining the inverter output voltage reference. For the unequal power sharing situation, the modification is before the voltage reference is formed. This means that when these two situations exist, the proposed strategies can be effective at the same time.

## VI. CONCLUSIONS

The influences of distribution lines on parallel inverters with the droop control method have been analyzed. It can be observed that the control coupling caused by the resistance in distribution lines reduces system stability. It can also be seen that unequally distributed reactive power is caused by the differences in the inductances of distribution lines. A control method, which produces a virtual negative resistive output impedance, is proposed to counteract the resistance in the distribution lines and a modified droop control method with indirect voltage control is proposed to make the power distribution equal. These control strategies have been validated by simulation and experimental results.

## APPENDIX I

Control equation (13) can be rewritten as (18).

$$U_n^{*2} + (2\pi f_n L_n I_n)^2 - 2U_n^* (2\pi f_n L_n I_n) \sin \varphi_n = U_{Ln}^{*2} \quad (18)$$

In the main circuit, shown in Fig.1, can be obtained on the basis of the KVL and KCL:

$$U_n^2 + (2\pi f_n L_n I_n)^2 - 2U_n (2\pi f_n L_n I_n) \sin \varphi_n = U_L^2 \quad (19)$$

$$U_L = NI_n Z_{Load} \quad (20)$$

Where  $Z_{Load} = \sqrt{R_{Load}^2 + (2\pi f_n L_{Load})^2}$ . Equation (20) is based on an assumption that the current is equally shared by parallel inverters.

The inverter output voltage loop is assumed to be equal to the first-order inertial link, which is:

$$U_n = \frac{1}{1 + Ts} U_n^* \quad (21)$$

Where T is the time constant of the voltage loop.

By substituting (19) (20) and (21) into (18) to eliminate  $I_n$ ,  $U_n^*$  and  $U_n$ , it is obtained that :

$$\frac{\sqrt{U_{Ln}^{*2} - U_L^2 C^2 \cos^2 \varphi_n}}{U_L \left( \left( \sqrt{1 - C^2 \cos^2 \varphi_n} + C \sin \varphi_n \right) Ts + \sqrt{1 - C^2 \cos^2 \varphi_n} \right)} \quad (22)$$

$$\text{Where: } C = \frac{2\pi f_n L_n}{NZ_{Load}}$$

In the steady state,  $s=0$ , which can be derived by:

$$U_{Ln0} = U_L \quad (23)$$

A small signal analysis is made of (22). Suppose that  $U_{Ln}^* = U_{Ln0}^* + \hat{u}_{Ln}^*$  and  $U_L = U_{L0} + \hat{u}_L$ . Substitute this into (22) with consideration of (23) and eliminate the high order small-signal term. Then it can be derived as:

$$\frac{\hat{u}_L}{\hat{u}_{Ln}^*} = \frac{1}{\left( 1 + C \sin \varphi_n \sqrt{1 - C^2 \cos^2 \varphi_n} - C^2 \cos^2 \varphi_n \right) Ts + 1} \quad (24)$$

## REFERENCES

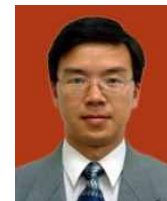
- [1] K. Siri, C. Q. Lee, and T. F. Wu, "Current distribution control for parallel connected converters part II," *IEEE Trans. Aerosp. Electron. Syst.*, Vol. 28, No. 3, pp. 841–851, Jul. 1992.
- [2] T.-F. Wu, Y.-K. Chen and Y.-H. Huang, "3C Strategy for Inverters in Parallel Operation Achieving an Equal Current Distribution," *IEEE Trans. Ind. Electron.*, Vol. 47, pp. 273-281, Apr. 2000.
- [3] Chen, J. F. and Chu, C. L., "Combination voltage controlled and current-controlled PWM inverter for UPS parallel operation," *IEEE Trans. Ind. Electron.*, Vol. 10, pp. 547-558, Sep. 1995.
- [4] U. Borup, F. Blaabjerg, and P. Enjeti, "Sharing of nonlinear load in parallel-connected three-phase converters," *IEEE Trans. Ind. Applicat.*, Vol. 37, No. 6, pp. 1817–1823, Nov./Dec. 2001.
- [5] Y. B. Byun, T. G. Koo, K. Y. Joe, E. S. Kim, J. I. Seo, and D. H. Kim, "Parallel operation of three-phase UPS inverters by wireless load sharing control," in *Proc. INTELEC*, pp. 526–532. Sep. 2000
- [6] J. Guerrero, J. Matas, L. G. de Vicuna, M. Castilla, and J. Miret, "Decentralized control for parallel operation of distributed generation inverters using resistive output

- impedance," *IEEE Trans. Ind. Electron.*, Vol. 54, No. 2, pp. 994–1004, Apr. 2007.
- [7] X. Zhang, J. Liu, T. Liu, and L. Zhou, "A novel power distribution strategy for parallel inverters in islanded mode microgrid," in *Proc. IEEE APEC'10 Conf.*, pp. 2116 - 2120, 2010.
- [8] J. M. Guerrero, L. García de Vicuña, J. Matas, M. Castilla, and J. Miret, "A wireless controller to enhance dynamic performance of parallel inverters in distributed generation systems," *IEEE Trans. Power Electron.*, Vol. 19, No. 5, pp. 1205–1213, Sep. 2004.
- [9] A. Tuladhar, H. Jin, T. Unger, and K. Mauch, "Control of parallel inverters in distributed AC power systems with consideration of the line impedance effect," in *Proc. IEEE APEC'98 Conf.*, pp. 321-328, 1998.
- [10] J. M. Guerrero, L. García de Vicuña, J. Matas, M. Castilla, and J. Miret, "Output impedance design of parallel-connected UPS inverters with wireless load-sharing control," *IEEE Trans. Ind. Electron.*, Vol. 52, No. 4, pp. 1126–1135, Aug. 2005.
- [11] S. J. Chiang and J. M. Chang, "Parallel control of the UPS inverters with frequency-dependent droop scheme," in *Proc. IEEE 32nd Power Electronics Specialists Conf.*, Vol. 02, pp. 957–961, 2001.
- [12] W. Yao, M. Chen, J. Matas, J. Guerrero, and Z.-M. Qian, "Design and analysis of the droop control method for parallel inverters considering the impact of the complex impedance on the power sharing," *IEEE Trans. Ind. Electron.*, Vol. 58, No. 2, pp. 576–588, Feb. 2011.
- [13] Qing-Chang Zhong, "Robust droop controller for accurate proportional load sharing among inverters operated in parallel," *IEEE Trans. Ind. Electron.*, Vol. 58, 2011, to appear.
- [14] K. De Brabandere, B. Bolsens, J. Van den Keybus, A. Woyte, J. Driesen, R. Belmans, and K. U. Leuven, "A voltage and frequency droop control method for parallel inverters," in *Proc. IEEE PESC*, Vol. 4, pp. 2501–2507, 2004.
- [15] Y. Li and Y. W. Li, "Decoupled power control for an inverter based low voltage microgrid in autonomous operation," in *Proc. IEEE IPEMC'09 Conf.*, pp. 2490- 2496, 2009.
- [16] C.-T. Lee, C.-C. Chu, and P.-T. Cheng, "A new droop control method for the autonomous operation of distributed energy resource interface converters," *IEEE Trans. Power Electron.*, Vol. 28, No. 4, pp. 1980–1993, Apr. 2013
- [17] J. Guerrero, J. Matas, L. de Vicuna, M. Castilla, and J. Miret, "Wireless-control strategy for parallel operation of distributed-generation inverters," *IEEE Trans. Ind. Electron.*, Vol. 53, No. 5, pp. 1461–1470, Oct. 2006.
- [18] Y. W. Li and C. N. Kao, "An accurate power control strategy for power electronics-interfaced distributed generation units operating in a low-voltage multibus microgrid," *IEEE Trans. Power Electron.*, Vol. 24, No. 12, pp. 2977–2988, Aug. 2009.
- [19] A. R. Bergen, *Power Systems Analysis. Englewood Cliffs*, NJ: Prentice-Hall, 1986.
- [20] E. A. A. Coelho, P. C. Cortizo, and P. F. D. Garcia, "Small-signal stability for parallel-connected inverters in stand-alone AC supply systems," *IEEE Trans. Ind. Appl.*, Vol. 38, No. 2, pp.533-542, Mar./Apr. 2002 .
- [21] M. T. Abuelma'atti, "An improved approximation of the transmission line parameters of overhead wires," *IEEE Trans. Electromagn. Compat.*, Vol. 32, No. 4, pp. 303-304, Nov. 1990.
- [22] F. Li, R. Broadwater, and A. Sargent, "Cable impedance calculations with parallel circuits and multi-neutral returns in distribution networks," *IEEE Power Engineering Society Winter Meeting*, Vol. 2, pp. 898-903, 2001.
- [23] N. Ishigure, K. Matsui, and F. Ueda, "Development of an on-line impedance meter to measure the impedance of a distribution line," in *Proc. ISIE'01*, Vol. 1, pp. 549–554, 2001.
- [24] H. Fu, Z. Zhou, X. Wei, and F. Tao, "Study on the measurement of power-transmission-line parameters with induced voltage," *China International Conference on Electricity Distribution*, pp. 1-6, 13-16, Sep. 2010.

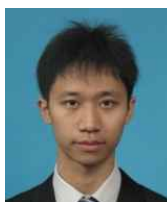


systems.

**Xuan Zhang** was born in China. He received his B.S. in Electrical Engineering from Xi'an Jiaotong University, Xi'an, China, in 2007. He is currently working toward his Ph.D. in Electrical Engineering at the same university. His current research interests include modeling and control of inverters in microgrids and distribution generation



**Jinjun Liu** was born in China. He received his B.S. and Ph.D. in Electrical Engineering from Xi'an Jiaotong University (XJTU), Xi'an, China, in 1992 and 1997, respectively. He then joined the School of Electrical Engineering XJTU as a faculty member. In 1998, he led the founding of the XJTU/Rockwell Automation Laboratory and served as the Lab Director. From 1999 until early 2002, he was with the Center for Power Electronics Systems at Virginia Polytechnic Institute and State University, Blacksburg, VA, USA, as a Visiting Scholar. He then returned to XJTU and in late 2002 was promoted to Full Professor and Head of the Power Electronics and Renewable Energy Center at XJTU. From 2005 to early 2010, he served as the Associate Dean for the School of Electrical Engineering at XJTU. He is currently serving as the Dean for Undergraduate Education at XJTU. He has coauthored 3 books, published over 100 technical papers, holds 8 patents, and has received several national, provincial or ministerial awards for scientific or career achievements. In 2006 he received the Delta Scholar Award. His current research interests include power quality control, renewable energy generation and utility applications of power electronics, and modeling and control of power electronic systems.



**Zhiyuan You** was born in China. He received his B.S. in Electrical Engineering from Xi'an Jiaotong University, Xi'an, China, in 2011. He is currently working toward his M.S. in Electrical Engineering at the same university. His current research interests include control of inverters in microgrids and distribution generation systems.



**Ting Liu** was born in China. She received her B.S. and M.S. in Electrical Engineering from Xi'an Jiaotong University, Xi'an, China, in 2009 and 2012, respectively. Her current research interests include power electronics and control, which include parallel inverter control, microgrids and distribution generation systems.